Ibn Al-Haitham Journal for Pure and Applied Sciences
Journal homepage: jih.uobaghdad.edu.iq
PISSN: 1609-4042, EISSN: 2521-3407
IHJPAS. 2025, 38 (1)

Development and Characterization of Chitosan Nanoparticles Loaded with Amoxicillin as Advanced Drug Delivery Systems against *Streptococcus Mutans*

Abdullah J Jasem[1*] and Maha A Mahmood[2]
[1,2]Department of Basic Sciences, College of Dentistry, University of Baghdad, Baghdad, Iraq.
*Corresponding Author.

Received: 17 May 2023 Accepted: 1 August 2023 Published: 20 January 2025
doi.org/10.30526/38.1.3501

Abstract

This study's primary objective was to create nanotechnology-based, precisely regulated drug delivery devices. Antibiotic Amoxicillin was chosen, and chitosan nanoparticles (CSNPs) were chosen to transport the medicine. Using the ionic gelation process, chitosan solution NPs were synthesized using tripolyphosphate (TPP). Antibiotic-loaded chitosan nanoparticles (CSNPs) were then used to create a nanocomposite with good performance. The resultant nanocomposite can be put to use as an effective, non-toxic antimicrobial agent. CMCS has a considerably wider range of uses as an anti-bacterial agent than chitosan since it is soluble in a wide pH range. Due to its water solubility, Ten *S. mutans* isolates were purified in two mediums, making it easy to use and elicit a variety of biological activities of CMCS in pharma and cosmetics. Tryptone yeast extract cysteine sucrose mitis salivarius bacitracin agar. MS colonies on MSBA plates were blue, spherical or ovoid, 1-2 mm in diameter, with elevated surfaces that stuck well to the agar. Rough colonies had a rough or frosted glass surface. Samples treated with chitosan, carboxymethyl chitosan, chitosan nanoparticles, and their nanocomposite containing antibiotics (Amoxicillin) stymied the growth of *Streptococcus mutans*. Chitosan nanoparticles and their loaded antibiotics were discovered by scanning Electron Microscopy (SEM) and Fourier transform infrared spectroscopy (FTIR). In addition, the cytotoxicity of both the nanocomposite and amoxicillin loaded on nano-chitosan were compared to that of amoxicillin alone. PH 4.5 with a drug/polymer ratio of 1:2 (w/v) resulted in 89.33% entrapment and 53% loading efficiency for Amoxicillin in terms of their particle size, surface charge, bond interaction, and shape, respectively. A zeta potential of +24.5 mV and an average particle size of 258 nm were found through analysis. The results showed the superior antibacterial efficacy of the AMX-CSNPs. It can be concluded that AMX-CSNPs and CSNPs displayed acceptable physicochemical characterizations, and effective antimicrobial activities

against *Streptococcus mutans***.** These formulations could enhance drug delivery for treating cariogenic bacteria causing dental caries.

Keywords: Chitosan nanoparticles CSNP, carboxymethyl chitosan CMC, Fourier-transform infrared spectroscopy FTIR, Polydispersity Index PDI, ζ –average Zeta potential.

1. Introduction

Dental caries (dental decay) can inflame, kill vital pulp tissue, and transmit infection to the tooth's periapex. Acidogenic plaque bacteria cause sickness (1). *S. mutans*, a crucial component of dental plaque, is often considered the foundation of the oral microbiota. Tooth decay (also known as "thetal caries") can cause inflammation and death of the pulp tissue, spreading infection to the tooth's periapex. Acidogenic plaque bacteria can lead to various illnesses (2). *S. mutans*, a crucial component of dental plaque, is often considered the foundation of the oral microbiota. Cariogenic bacteria like *Streptococcus* and *Lactobacillus* produce lactic acid during carbohydrate fermentation, lowering the local pH below the threshold value and demineralizing the tooth surface(47,48). Nanomaterials' compact size and high surface area per unit mass improves solution binding and dispersibility. Its antibacterial properties come from binding with proteins, plaque, and harmful bacteria. Nanoparticles' size and high surface-to-volume ratio may make them antimicrobial (46). They should interact closely with bacterial membranes to produce an antibiotic effect (3). Metallic and other nanoparticles combined with polymers and other base materials can be placed onto surfaces for antibacterial and anti-adhesive purposes (4, 5). Biomedical applications use chitosan because it is nontoxic, biocompatible, and antimicrobial. Deacetylating crustacean exoskeleton chitin produces the biopolymer chitosan. Positively charged chitosan dissolves in acidic to neutral liquids and sticks to mucosal surfaces. Regional medicine distribution may use chitosan nanoparticles (6). Chitosan is a cationic polymer made up of N-acetylglucosamine and glucose amine in a repeating structure. Protein carriers, drug administration, and wound healing are only some of the biological uses that could benefit from this material's biocompatibility, biodegradability, and nontoxicity (7-8). CSNPs excel in these areas due to their size, shape, and zeta potential. CSNPs can transport drugs (9, 10), vaccinations (11, 12), and even genes (13, 14). Studies have shown that chitosan nanoparticles are more effective than chitosan itself at eliminating bacteria and viruses (19). Slowly releasing medicines from chitosan nanoparticles may increase their solubility, stability, effectiveness, and toxicity (15, 16). Chitosan nanoparticles can be made in a number of ways (17). These include molecular self-assembly, template polymerization, reverse micelle, and emulsion cross-linking. When deciding on a preparation process, it is important to consider particle size, heat and chemical stability, as well as the stability of the finished product (18).

The study's objective is to investigate whether chitosan-based nanoparticles could improve antimicrobial treatment. Many antimicrobial treatments are less effective when they can't get into cells. Some antibiotics, like amoxicillin, can be used without side effects to treat cariogenic bacterial infections better.

2. Materials and Methods

Chemicals used as analytical reagents were not purified. Merck Chemical Co. provided chitosan (MW = 60-120 kDa, deacetylation degree 85%), TPP, glacial acetic acid, and amoxicillin. Absorbance was measured using a PerkinElmer Lambda 25 spectrometer (Waltham, MA, USA). Morphological examination using SEM (TESCAN, MIRA III) was performed. Spectra were obtained using an FTIR spectrophotometer (Termo, AVATAR). The size distribution of NPs was determined using a Zetasizer Nano ZS dynamic light scattering spectrophotometer (Malvern Instruments, Malvern, UK). Solar energy produces Carboxymethyl Chitosan. Weight 220, Formula: C8H14NO6 Around 80% of the time, you can substitute.

By letting 100 mg of CS dissolve in 100 mL of 1% acetic acid at room temperature overnight, the mixture was filtered using a 0.45 millimeter syringe filter. The addition of the ice cold TPP solution to the heating CS solution mixture resulted in the spontaneous generation of CSNPs. The synthesis of CSNPs was evidenced by opalescence in cloudy solutions. CSNPs were synthesized at pH 3.5, 4.5, 5.0, and 5.5 with CS to TPP mass ratios of 3 to 1, 4 to 1, and 5:1, respectively, and then analyzed by DLS. AMX was added to a solution of CSNPs at various drug/polymer ratios (1:1, 1:2, 1:3, 2:1, and 3:1) to create drug-loaded nanoparticles. The nanoparticle suspensions were centrifuged at 18,000 rpm for 30 minutes after being agitated for 1 hour. Pellets were lyophilized and stored to evaluate drug loading efficiency. AMX-CSNPs solution free Amoxi was calculated by monitoring absorbance at 317 nm. We compared two AMX standard curves. The comparison of two AMX standard curves was performed to ensure accuracy in determining free AMX concentration in the CSNPs solution, as monitored by absorbance at 317 nm (19).

2.1 AMX+CSNPs: A Characterization

Zetasizer Nano ZS (Malvern Instruments, UK) was used to determine particle size and zeta potential. The He-Ne 633 nm laser was used to take the measurements at room temperature (25 °C). Overnight at room temperature, stabilization and sonication were performed on samples before measurements (19). DLS analysis was used to determine the size of the particles and surface charge of CSNPs synthesized at several pH levels (3.5, 4.5, 5.0, and 5.5) using CS to TPP mass ratios of 3:1, 4:1, and 5:1.

2.2 Fourier-transform infrared spectroscopy (FTIR):

FTIR of intact CLM, NPs, and physical mixture were obtained from FTIR spectrophotometer: model (Teramo, AVATAR) Spectra were obtained by ATR technique. The scanning range was 4000-400 cm-1 (19).

2.3 Scanning Electron Microscopy (SEM):

The nanoparticles' morphology was studied with scanning electron microscopy (SEM). After being air-dried at ambient temperature, the NPs were sputter coated with gold, mounted on metal stubs with adhesive tape, and examined using a scanning electron microscope (TESCAN, MIRA III) under high vacuum at an acceleration voltage of 20 kV.

2.4 Drug entrapment study

Nanoparticle yield is the theoretical weight of the polymer and medicine used minus the nanoparticle weight. After dispersing nanoparticles by weight in 10 ml of PBS (pH 7.4), incubating

for 25 minutes, and centrifuging at 19000 rpm for 20 minutes, the encapsulation efficiency was calculated. Amoxicillin absorbance of 247 nm was found in the supernatant. Amoxicillin loading capacity (L.C.) and amoxicillin encapsulation efficiency (A.E.E.) of the nanoparticles were determined using the following formulas. (19)

Entrapment efficiency = (Drug Total − Drug free)/Drug total × 100

Loading capacity = (Drug Total − Drug free)/Weight of the nanoparticles × 100

2.5 Assay Cytotoxicity for Nano chitosan, amoxicillin and amoxicillin loaded chitosan nano particles

The study investigates the growth and extracts of MCF-7 breast cancer cells. MTT assesses cell viability. A 24-hour 96-well plate experiment seeded 10,000 MCF-7 cells. Cells received different extracts after 24 hours. Cell viability was assessed after medium removal using MTT (5 g/L in PBS, pH 7.4) for 4 hours. Active cells precipitate MTT-soluble DMSO-soluble formazan. After gently shaking the plate to disperse the precipitate, absorbance was 570 nm instead of 630. Stable absorbance showed cell viability. Linear regression determined the extracts' 50% median lethal concentration (LC50), which halves cell viability. MCF-7 cells are seeded into a 96-well plate, treated with different extracts, assessed for viability using the MTT assay, and estimated for LC50s using linear regression analysis (20).

3. Results

Amoxicillin-CSNPs had their drug loading and encapsulation efficiency maximized out using spectrophotometry. To quantify the amoxicillin loaded into CSNPs, the derivative o-Phthaldialdehyde Reagent was utilized to observe a shift in absorbance at 340 nm. Maximum encapsulation (89.33 2.7%) and loading efficiency (53.2 2.4) were observed in the formulation containing amoxicillin-CSNPs at a ratio of 1:2. Using dynamic light scattering, the hydrodynamic size and surface charge of CSNPs/AMOXICILLIN CSNPs in an aqueous media were determined. The poly-dispersity index for AMX-CSNPs was 0.19, and their average particle size was 258 nm (**Figure 2a**). For efficient medication distribution, it is crucial to pay attention to particle size and surface charge. Zeta analysis reveals the size distribution of the produced nanoparticles in **Figure 3(A)**. AMX-NP's mean particle size is 258 nm.

Table 1. UV-visible spectrophotometer analysis of AMX-CSNPs encapsulation and loading effectiveness. Mean standard deviation (n = 3).

CSNPs: AMX ratio	Encapsulation efficiency (%) wt	Drug loading (%) wt	Particle size	Polydispersity Index PDI	Zeta potential
1:1	69.05 ± 1.35	27 ± 2.2	237 ± 33.1	0.65	10.5 ± 4.4
1:2	89.33 ± 2.7	53 ± 2.4	258 ± 46.5	0.19	24.5 ± 4.8
1:3	85.28 ± 3.1	42 ± 1.9	314 ± 45.9	0.38	18.3 ± 4.8
2:1	38.54 ± 2.8	29 ± 2.3	368 ± 23.9	0.32	15.8 ± 4.8
3:1	39.39 ± 6.5	26 ± 1.6	289 ± 5.8	0.44	14.4 ± 4.9

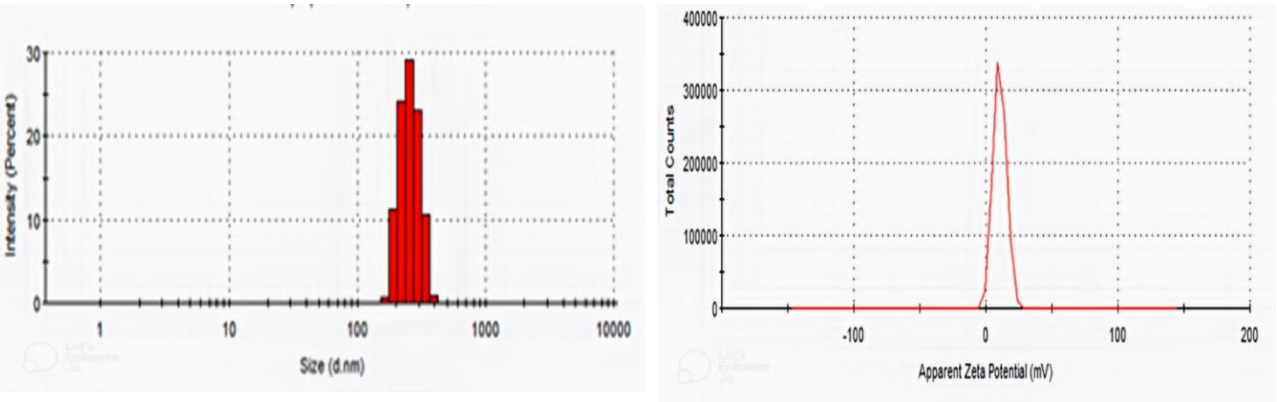

Figure 1. Employing the Zetasizer Nano ZS, we determined the particle size distribution and Zeta potential value of various CSNPs to characterize their size and surface charges. A 2:1 Amoxi ratio

3.1 Fourier Transform Infrared (FT-IR) analysis

The interaction between CS and Amoxicillin which confirms the encapsulation of Amoxicillin into the Nano carrier. Was identified by using FT-IR Technique:

In the image below, we can see the FTIR spectra of CSNPs, AMX, and AMX-CSNPs. CSNPs showed a peak at 3500 cm1, consistent with the NH vibrational frequency, while AMX-CSNPs red-shifted to 3446 cm1, possibly due to the hydroxyl stretch (-OH). It is normal for C-H stretch vibrations to exhibit a peak at 2925 cm1. N-H bending in the NP causes a peak at 1627 cm1 that is red-shifted to 1634 cm1 in drug-loaded nanoparticles. We observed peaks at 1540 and 1558 cm1 due to the N-H bending of the amine in amoxicillin-specific nuclear peptides (-CSNPs). The drug's strong peak at 1053 cm1 and red shifts to 1098 cm1 were both caused by C-O stretching. Finally, we observed an 897 cm1 change in C-H out-of-plane bending. As a result, we know that CSNPs are loaded with AMX.

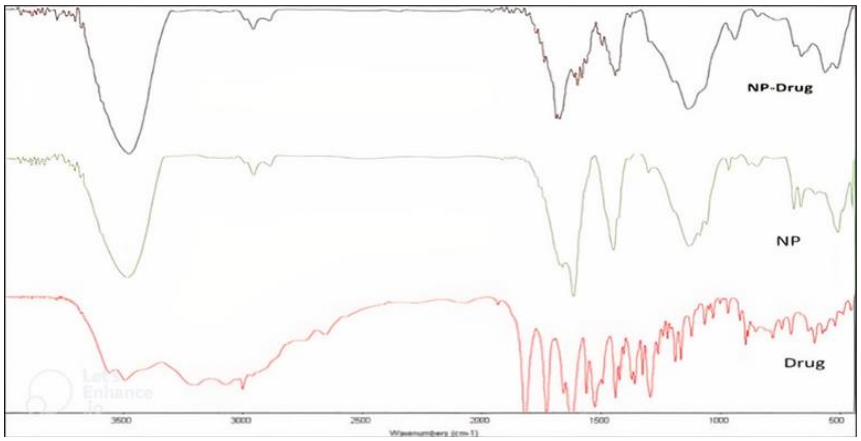

Figure2: FTIR spectra of CSNPs (green), Amoxicillin (red), AMX-CSNPs (black)

3.2 Morphology

Figure 3 displays the SEM of amoxicillin-loaded chitosan nanoparticles. The size of the particles fell within the nanoscale range, exhibiting a relatively spherical and regular form. We confirmed that the particles fall within the nanoscale range, possessing a smooth surface texture and a regular spherical shape.

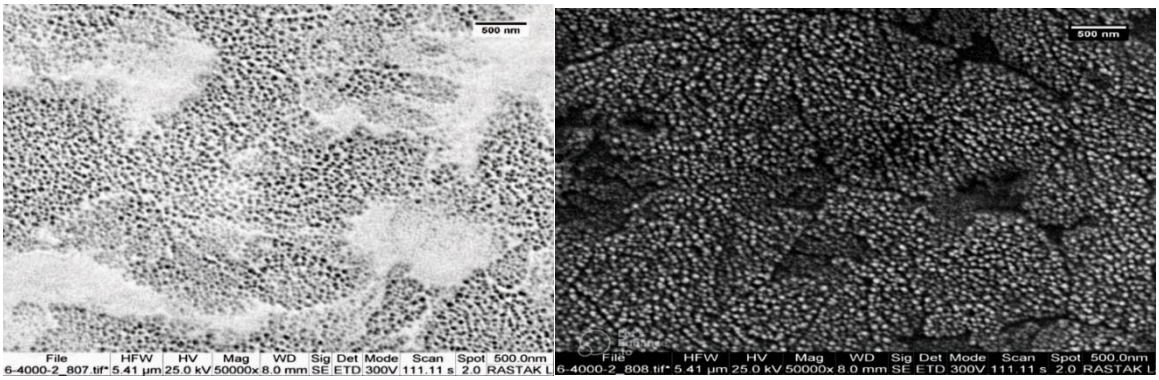

Figure 3: SEM showing chitosan nanoparticles loaded with chitosan nanoparticles

3.3 The MTT cell viability assay for cytotoxicity testing

The statistical analysis demonstrated no significant cell inhibition with varied concentrations of chitosan nanoparticles, amoxicillin, and amoxicillin-loaded Nano Chitosan with TPP. The study materials are safe and non-toxic to MCF-7 breast cancer cells at various doses. Table 2 and **Figure 3** a,b,c showMCF-7 cell cytotoxicity of chitosan nanoparticles, amoxicillin, and amoxicillin-loaded Nano Chitosan. The graphic shows that cell viability remained unaffected at all concentrations. This suggests that these materials are safe for cancer treatment and do not harm breast cancer cells. **Figures 3** (B, C, D, and E) exhibit blue fluorescence staining (Hochst) of active nucleus cells. Image (b) shows breast cancer cell viability before therapy. Images (C-E) show MCF-7 cells that survived treatment with chitosan nanoparticles and amoxicillin-loaded Nano Chitosan with TPP at 16 to 250 µg/ml. Using pictures b to e, chitosan nanoparticles and amoxicillin-loaded Nano Chitosan with TPP were non-cytotoxic. Thus, they may be used as antibacterial and antifungal drugs in organs without harming healthy or sick cells. They can also fight oral infection-causing germs.

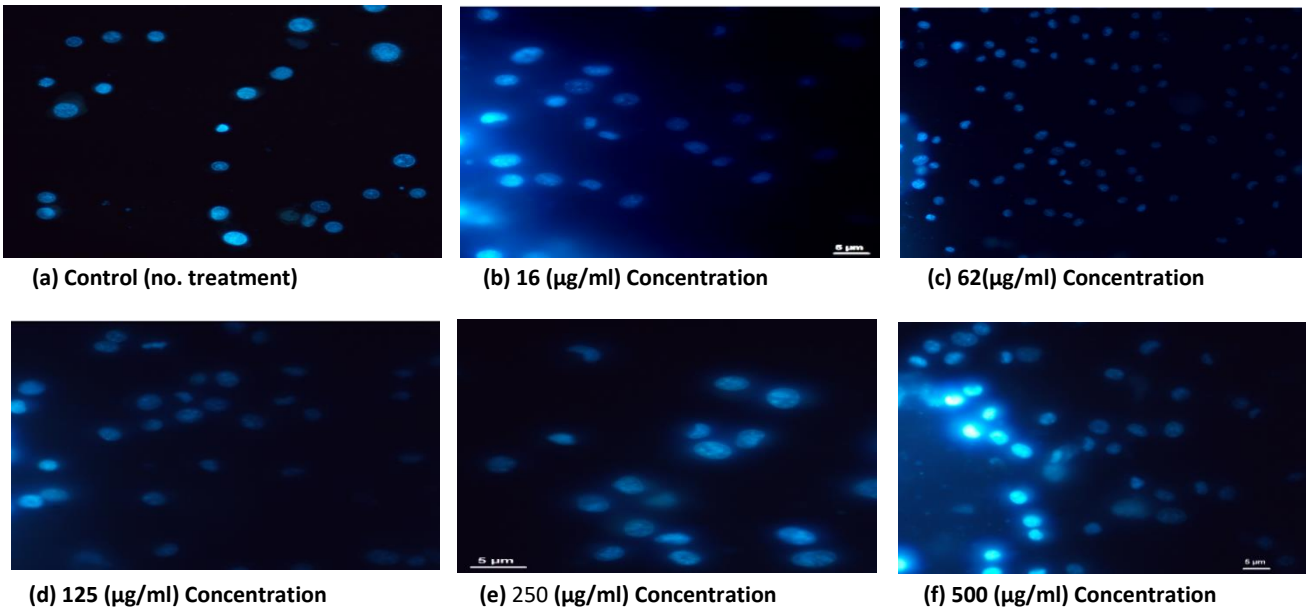

Figure 4. Relative cell viability of Amoxicillin loaded chitosan nanoparticles (a) Control (no. treatment), (b) 16 (µg/ml), (C) 62(µg/ml), (d) 125 (µg/ml), (e) 250 (µg/ml), (f) 500 (µg/ml).

Table 2. Show The MTT cell viability assay for cytotoxicity testing

The MTT cell viability assay for cytotoxicity testing												
	Amoxicillin				*Amoxicillin + CSNP*					*CSNP*		
conc. (µg/ml)	z	SD	Viability	SD	Average	SD	Viability	SD	Average	SD	Viability	SD
500	1.412	0.078	101.2	5.613	1.392	0.049	96.99	3.433	1.4091	0.0268	101.075	1.9291
		259	791	285	667	298	362	388	67	95	9	44
250	1.428	0.035	102.4	2.574	1.383	0.073	96.32	5.149	1.3833	0.0222	99.2229	1.5972
	333	887	507	072		935	037	282	33	68	5	31
125	1.404	0.038	100.7	2.796	1.350	0.044	94.08	3.098	1.3443	0.0268	96.4255	1.9223
	5	986	412	358	833	486	009	241	33		8	31
62	1.354	0.030	97.16	2.180	1.320	0.024	91.97	1.722	1.3103	0.0335	93.9868	2.4097
	667	395	677	168	667	736	911	758	33	96	5	29
31	1.414	0.036	101.4	2.633	1.301	0.028	90.62	2.006	1.304	0.0292	93.5325	2.0946
		721	226	872	167	806	101	199		0274	7621	37628
16	1.435	0.023	102.9	1.664	1.306	0.023	91.00	1.654	1.3871	0.0235	99.4979	1.6860
	667	209	767	736	667	754	406	391	66667	06737	0795	77941
Con	1.394	0.038	100	2.734	1.435	0.058	100	4.087	1.3941	0.0381	100	2.7340
trol	167	118		092	833	69		552	67	18		92

3.4 Isolation of *S.mutans*

Ten *S.mutans* isolates were purified in two mediums. Tryptone yeast extract cysteine sucrose mitis salivarius bacitracin agar Bacitracin Agar. The blue, spherical or ovoid, 1-2 mm in diameter MS colonies on MSBA plates had raised surfaces that adhered well to the agar. The surface of rough colonies was rough or frosted glass. While smooth colonies were spherical. Most MS colonies had a dip in the middle with a polysaccharide drop, although others were completely immersed (**Figure 5**).

Figure 5. (a) *S.mutans and colonies on Mitis Salivarius Bacitracin agar* (b) *S.mutans* colonies on TYCSB selective agar.

3.5 The Anti-Bacterial Activity of different chitosan compounds against *S. mutans*

By measuring the mean inhibition zone diameters of the ten bacterial isolates in mm using a ruler, we were able to estimate the antibacterial activities of chitosan, carboxymethyl chitosan, chitosan nanoparticles, amoxicillin loaded on chitosan nanoparticles, and amoxicillin.

Table 3. Values of inhibition zone for the five groups of compounds against *Streptococcus mutans*.

Compound	Conc. (Mg/ml)	Min	Max	Mean	SD	F-Test	P-Value
Cs	10	15	17	15.86	0.76	304.672	0
	5	12	13.65	12.74	0.54		
	2.5	10.5	12.32	10.93	0.66		
	1.25	8.5	10.5	9.05	0.69		
	0.625	6	7.59	6.69	0.5		
CMC	10	15.5	18.32	16.49	0.96	219.907	0
	5	13	14.44	13.34	0.51		
	2.5	10	12.5	11.5	0.78		
	1.25	9	11.86	9.69	0.94		
	0.625	6	7.88	6.82	0.59		
CSNPs	10	18	21.5	19.14	1.12	298.81	0
	5	15	16.6	15.63	0.53		
	2.5	12	14.39	13.28	0.75		
	1.25	9.5	11.85	10.59	0.91		
	0.625	7	8.5	7.74	0.56		
AMX + CSNPs	10	24	29	26.41	1.79	131.759	0
	5	20.1	26	22.9	2.33		
	2.5	16.32	20.3	18.12	1.33		
	1.25	13	17	15	1.13		
	0.625	9.5	12.63	11.66	1.3		
AMX	10	19	24.7	22.17	1.86	157.139	0
	5	15.4	20.5	18.59	1.46		
	2.5	12.8	16.5	15.72	1.14		
	1.25	10.18	13.6	12.64	0.97		
	0.625	8	10	8.93	0.76		

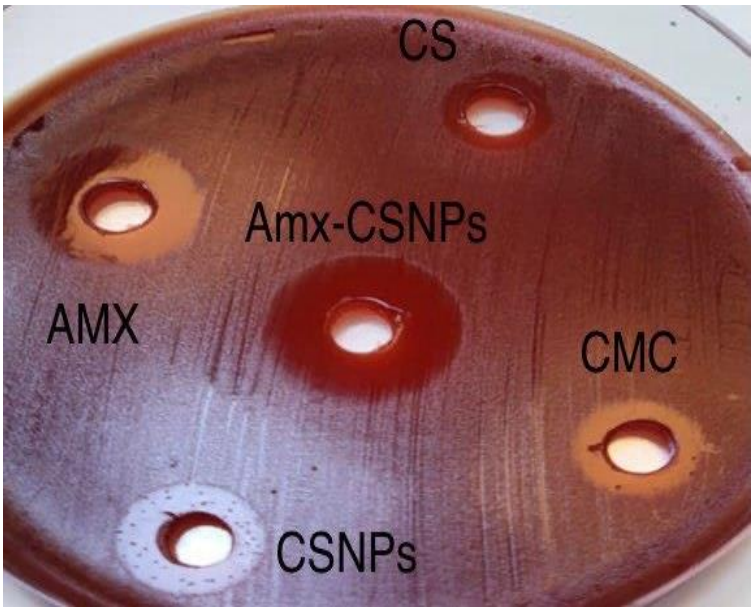

Figure 6. The inhibition zone (IZ) of *S. mutans* isolates against five compound (CS, CSNPs CMC, Amoxicillin loaded on CSNPs, Amoxicillin)

Parameter	compound	No	Minimum	Maximum	Median	p-value
MIC	Chitosan	10	2.5	2.5	2.5	0.000
	CMC	10	2.5	2.5	2.5	
	CSNPs	10	1.25	2.2	2.5	
	AMX	10	1.25	1.25	1.25	
	AMX+CSNPs	10	0.625	0.625	0.625	
MBC	Chitosan	10	5	5	5	0.000
	CMC	10	5	5	5	
	CSNPs	10	2.5	5	5	
	AMX	10	2.5	2.5	2.5	
	AMX+ CSNPs	10	0.625	0.625	0.625	
MBC\MIC	Chitosan	10	2	2	2	0.000
	CMC	10	2	2	2	
	AMX	10	2	4	2	
	CSNPs	10	2	2	2	
	AMX+ CSNPs	10	1	1	1	

Table 4. Values of MIC and MBC for the five groups of compounds against *Streptococcus mutans.*

4. Discussion

Chitosan, a cationic biocide used for external cleaning, was used in our study because it attacks bacterial cell membranes. Sudarshan et al. found that chitosan's amino group binds to bacterial surface components and limits their growth. At lower concentrations, chitosan may have adhered to the negatively charged bacterial surface, causing the cell membrane to rupture and release internal components, killing the cell. It's possible that a chitosan coating on the bacteria prevented them from leaking their internal ingredients and stopped the transfer of large amounts of mass across the cell membrane. Partially deacetylating chitin produces chitosan, a biopolymer with applications in the food, pharmaceutical, and chemical industries (21, 22). Antimicrobial chitosan prevents cavities (22). Chitosan is a nanoscale antibacterial, medication, gene, vaccine, and anti-tumor agent. Modified chitosan derivatives like CMC have increased antibacterial activity (23–24). Because chitosan is insoluble above pH 6.5, it is only bactericidal in acidic environments. Water-soluble, acidic-, and basic-soluble chitosan derivatives may be acceptable for the polycationic biocide (25). Because CMCS is pH-soluble, it is more antimicrobial than chitosan. Water solubility makes CMCS an appealing complexation agent for medicinal and cosmetic purposes. Water-soluble chitosan compounds were harmful to cancer cells but not to normal cells (26, 27). Since dentists recommend amoxicillin for mouth infections, we put it on nanochitosan.

Amoxicillin enhances oral microbiota resistance. We observed an increase in oral streptococci resistant to amoxicillin (28).

The CS/TPP ratio has an impact on the size and biology of CS nanoparticles (37). This study found that ion-charge interactions resulted in the best size distribution at 4:1 CS/TPP. Drug-loaded nanoparticles were produced. PH reduced the average chitosan NP particle size. PH and ionic strength (38). Tsai et al. studied CS/TPP nanoparticle size and storage solution ph. Nanoparticles shrank as pH increased. Based on the findings, the optimal size distribution was achieved at a CS/TPP ratio of 4:1 due to ion-charge interactions. The nanoparticles produced were loaded with drugs. The average size of chitosan nanoparticles was decreased by pH and ionic strength. Tsai and colleagues researched the effect of nanoparticle size and storage solution pH in CS/TPP. Tsai and colleagues examined the effect of storage solution pH on the size of CS/TPP nanoparticles. They found that nanoparticles decreased in size, leading to a reduction in the overall increase. Additionally, high drug concentrations during gel formation resulted in decreased interaction between CS and TPP, leading to the formation of larger particles. AMOXI-CSNPs are less homogeneous than interfacial depositions. All formulations showed a low PDI (0.4) and size variation. From 0 to 1, PDI measures mixture molecule or particle size heterogeneity. PDI values that are above 0.5 indicate significant heterogeneity (39).

Zeta potential has an impact on nanoparticle stability and mucoadhesivity (40). Gel-formed protonated amine groups increased zeta potential. Studies show that nanoparticles with higher zeta potentials are more stable. Electrostatic repulsion disperses charged particles (40). Long-chain amino groups in CS make a big electrical double layer that soaks up TPP anionic groups and stops them from sticking together (22). Increasing formulation CS/D ratios does not improve loading efficiency. Nanoparticle size, without aggregation, improved amoxicillin loading in CSNP solutions at pH 4.5. Precipitation occurred as the CS solution pH rose over 5.0, notably around 6.5. If its pH is below pH 4.2, chitosan's hydrogen ions partially neutralize TPP's hydroxide ions. Hydroxide ions do not deprotonate chitosan. Tripolyphosphoric ions connect protonated amino groups despite intramolecular electrostatic repulsion (30). PH impacts nanoparticle size. Table 2 demonstrates the spectrophotometrically calculated maximum drug loading and encapsulation effectiveness of Amoxicillin-CSNPs. The 1:2 Amoxicillin-CSNP formulation achieved the highest encapsulation and loading efficiencies, 89.33 2.7% and 53 2.4%, respectively. Increased amoxicillin or CSNP ratios reduce drug loading and encapsulation efficiency. Research supports these conclusions. (41, 42) The hydrodynamic size and surface charge. As drug loading increases the particle size, the amoxicillin amine group may cross-link with CSNPs. Shielding widens the particle size range, thereby reducing electrostatic attraction and elevating electrolyte ions, ultimately leading to a decrease in the water layer on the surface (30). Shielding particles reduces electrostatic contact, increases electrolyte ions, and thins the surface hydration layer (30). AM's amino group boosted amoxicillin-CSNPs' zeta potential to +24.5 mV. Residual amine groups boosted gentamicin-loaded CSNPs' zeta potential (43). Positive ions increased amoxicillin-CSNPs' zeta potential, stability, and antibacterial activity. Amoxicillin-CSNPs' stability showed that their surface has a large electric charge, which repels aggregation. Zhang et al. (44) believe that a big

positive potential minimizes particle agglomeration. SEM investigated amoxicillin-CSNP morphology. The amoxicillin-CSNPs were spherical at 200–300 nm. These may have influenced grouping. Drying lowers particle size, raises specific surface energy, and boosts CS hydrogen bond interaction, which may have promoted amoxicillin-CSNP clustering. In amoxicillin-CSNPs (30), the hydrogen bond interaction dominates drying. Particles gravitate without resistance. The zeta potential is constant above -30 mV or +30 mV (23). CSNPs are cationic because of the biopolymer's amino groups. Concentration increased chitosan viscosity, lowering drug encapsulation. Ionic drug-polymer interactions may capture nanoparticle drugs.

5. Conclusion

The AMX-CSNP preparation method is used. The CSNPs were made using a 4:1 CS to TPP ratio at a pH of 4.5. The M 1:2 formulations of CSNPs demonstrated maximum treatment effectiveness. Drug capsules. FTIR was used to detect AMX-CSNP bonding. Based on zeta potential measurements of +24.5 mV, DLS studies found that the average size of AMX-CSNPs was 258 nm. AMX-CSNPs exhibited both elemental analyses and dispersed spherical nanoparticles in experiments with *S. mutans,* AMX-CSNP demonstrated greater effectiveness than AMX alone. By enhancing AMX's antibacterial properties, CSNPs help AMX to better penetrate the bacterial cell membrane despite the presence of exotoxins. Finally, AMX-CSNPs did not kill MCF-7 cells in vitro. These findings suggest that AMX-CSNPs can enhance the therapeutic efficacy of AMX and facilitate the delivery of medications against cariogenic infections.

Acknowledgment

Many thanks to the Department of Basic Sciences, College of Dentistry, University of Baghdad, for their invaluable assistance in facilitating the practice sections of this article. Also, I would like to sincerely thank and express my great appreciation and heartfelt gratitude to “ALzahraa Jabbar Jasiem” for her scientific guidance, recommendations, advice, and support.

Conflict of Interest

The authors declare that they have no conflicts of interest.”

Funding

There is no funding for the article.

Ethical Clearance

The study was conducted in accordance with the ethical principles. It was carried out with patients verbal and analytical approval before the sample was taken. The study protocol and the subject information and consent form were reviewed and approved by Baghdad University, College of dentistry a local ethics committee according to the document number Ref. Number 404 and project No. 404821 on 27/December/2021 to get this approval.

References

1. Cushing BL, Kolesnichenko VL, O'Connor CJ. Recent advances in the liquid-phase syntheses of inorganic nanoparticles. Chem Rev. 2004;104(10):3893–3946. https://doi.org/10.1021/cr030027b.
2. Marsh PD, Martin MV. Oral Microbiology. 5th ed. London: Butterworth Heinemann; 2010.
3. Allaker RP, Douglas CWI. Non-conventional therapeutics for oral infections. Virulence. 2015;6(3):196–207. https://doi.org/10.4161/21505594.2014.983783.
4. Monteiro DR, Gorup LF, Takamiya AS, Ruvollo-Filho AC, de Camargo ER, Barbosa DB. The growing importance of materials that prevent microbial adhesion: Antimicrobial effect of medical devices containing silver. Int J Antimicrob Agents. 2009;34(2):103–110. https://doi.org/10.1016/j.ijantimicag.2009.01.017.
5. Hannig M, Kriener L, Hoth-Hannig W, Becker-Willinger C, Schmidt H. Influence of nanocomposite surface coating on biofilm formation in situ. J Nanosci Nanotechnol. 2007;7(12):4642–4648. https://doi.org/10.1166/jnn.2007.18117.
6. Wu Y, Yang W, Wang C, Hu J, Fu S. Chitosan nanoparticles as a novel delivery system for ammonium glycyrrhizinate. Int J Pharm. 2005;295(1–2):235–245. https://doi.org/10.1016/j.ijpharm.2005.01.042.
7. Rinaudo M. Chitin and chitosan: Properties and applications. Prog Polym Sci. 2006;31(7):603–632. https://doi.org/10.1016/j.progpolymsci.2006.06.001.
8. Ibrahim HM, Reda MM, Klingner A. Preparation and characterization of green carboxymethylchitosan (CMCS)-polyvinyl alcohol (PVA) electrospun nanofibers containing gold nanoparticles (AuNPs). Int J Biol Macromol. 2020;151:821–829. https://doi.org/10.1016/j.ijbiomac.2020.02.174.
9. Li HP, Qin L, Wang ZD. Synthesis and characterization of ramose tetralactosyl-lysyl-chitosan-5-fluorouracil and its in vitro release. Res Chem Intermed. 2012;38(6):1421–1429. https://doi.org/10.1007/s11164-011-0473-x.
10. Borges O, Tavares J, de Sousa A, Borchard G, Junginger HE, Cordeiro-da-Silva A. Evaluation of the immune response following a short oral vaccination schedule with hepatitis B antigen encapsulated into alginate-coated chitosan nanoparticles. Eur J Pharm Sci. 2007;32(4–5):278–290. https://doi.org/10.1016/j.ejps.2007.08.005.
11. Gan Q, Wang T, Cochrane C, McCarron P. Modulation of surface charge, particle size, and morphological properties of chitosan-TPP nanoparticles. Colloids Surf B Biointerfaces. 2005;44(2–3):65–73. https://doi.org/10.1016/j.colsurfb.2005.06.001.
12. Stanić V, Dimitrijević S, Antić-Stanković J, Mitrić M, Jokić B, Plećaš IB, Raičević S. Synthesis, characterization, and antimicrobial activity of copper and zinc-doped hydroxyapatite nanopowders. Appl Surf Sci. 2010;256(20):6083–6089. https://doi.org/10.1016/j.apsusc.2010.03.124.
13. Martinez-Gutierrez F, Olive PL, Banuelos A, Orrantia E, Nino-Martinez N, Martinez-Castanon GA, Ruiz F. Evaluation of antimicrobial and cytotoxic effect of silver and titanium nanoparticles. Nanomedicine. 2010;6(5):681–688. https://doi.org/10.1016/j.nano.2010.02.001.
14. Lellouche J, Kahana E, Elias S, Gedanken A, Banin E. Antibiofilm activity of nanosized magnesium fluoride. Biomaterials. 2009;30(30):5969–5978. https://doi.org/10.1016/j.biomaterials.2009.07.012.
15. Jasem AJ, Mahmood MA. Preparation and characterization of amoxicillin-loaded chitosan nanoparticles. J Emerg Med Trauma Acute Care. 2023;2023(3):10. https://doi.org/10.5339/jemtac.2023.midc.10.
16. Mosaad RM, Alhalafi MH, Emam EA, Ibrahim MA, Ibrahim H. Enhancement of antimicrobial and dyeing properties of cellulosic fabrics via chitosan nanoparticles. Polymers (Basel). 2022;14(19):4211. https://doi.org/10.3390/polym14194211.

17. Matalqah SM, Aiedeh K, Mhaidat NM, Alzoubi KH, Bustanji Y, Hamad I. Chitosan nanoparticles as a novel drug delivery system: A review article. Curr Drug Targets. 2020;21(15):1613–1624. https://doi.org/10.2174/1389450121666200711172536.
18. Agnihotri SA, Mallikarjuna NN, Aminabhavi TM. Advances on chitosan-based micro- and nanoparticles in drug delivery. J Control Release. 2004;100(1):5–28. https://doi.org/10.1016/j.jconrel.2004.08.010.
19. Kumar GV, Su CH, Velusamy P. Kanamycin-chitosan nanoparticles to improve antibacterial activity against pathogens. J Taiwan Inst Chem Eng. 2016;65:574–583. https://doi.org/10.1016/j.jtice.2016.04.008.
20. Herdiana Y, Wathoni N, Shamsuddin S, Muchtaridi M. Cytotoxicity enhancement with chitosan delivery of α-Mangostin. Polymers (Basel). 2022;14(15):3139. https://doi.org/10.3390/polym14153139.
21. Iyakulawat P, Praphairaksit N, Chantarasiri N, Muangsin N. Preparation and evaluation of chitosan/carrageenan beads for controlled release of sodium diclofenac. AAPS PharmSciTech. 2007;8(4): E97. https://doi.org/10.1208/pt0804097.
22. Avadi MR, Sadeghi AM, Mohammadpour N, Abedin S, Atyabi F, Dinarvand R, Rafiee-Tehrani M. Preparation and characterization of insulin nanoparticles using chitosan and Arabic gum with ionic gelation method. Nanomedicine. 2010;6(1):58–63. https://doi.org/10.1016/j.nano.2009.04.007.
23. Jayakumar R, Nwe N, Tokura S, Tamura H. Sulfated chitin and chitosan as novel biomaterials. Int J Biol Macromol. 2007;40(3):175–181. https://doi.org/10.1016/j.ijbiomac.2006.06.021.
24. Yang TC, Chou CC, Li CF. Antibacterial activity of N-alkylated disaccharide chitosan derivatives. Int J Food Microbiol. 2005;97(3):237–245. https://doi.org/10.1016/S0168-1605(03)00083-7.
25. Li Z, Zhuang X, Liu X, Guan Y, Yao F. Study on antibacterial O-carboxymethylated chitosan/cellulose blend film from LiCl/N,N-dimethylacetamide solution. Polymer. 2002;43(5):1541–1547. https://doi.org/10.1016/S0032-3861(01)00699-1.
26. Je JY, Cho YS, Kim SK. Cytotoxic activities of water-soluble chitosan derivatives with different degree of deacetylation. Bioorg Med Chem Lett. 2006;16(8):2122–2126. https://doi.org/10.1016/j.bmcl.2006.01.060.
27. Qi L, Xu Z, Jiang X, Li Y, Wang M. Cytotoxic activities of chitosan nanoparticles and copper-loaded nanoparticles. Bioorg Med Chem Lett. 2005;15(5):1397–1399. https://doi.org/10.1016/j.bmcl.2005.01.010.
28. Ready D, Lancaster H, Qureshi F, Bedi R, Mullany P, Wilson M. Effect of amoxicillin use on oral microbiota in young children. Antimicrob Agents Chemother. 2004;48(8):2883–2887. https://doi.org/10.1128/AAC.48.8.2883-2887.2004.
29. Zhang H, Oh M, Allen C, Kumacheva E. Monodisperse chitosan nanoparticles for mucosal drug delivery. Biomacromolecules. 2004;5(6):2461–2468. https://doi.org/10.1021/bm0496211.
30. Fan W, Yan W, Xu Z, Ni H. Formation mechanism of monodisperse, low molecular weight chitosan nanoparticles by ionic gelation technique. Colloids Surf B Biointerfaces. 2012;90:21–27. https://doi.org/10.1016/j.colsurfb.2011.09.042.
31. Biswaro LS, da Costa Sousa MG, Rezende TMB, Dias SC, Franco OL. Antimicrobial peptides and nanotechnology: Recent advances and challenges. Front Microbiol. 2018;9:855. https://doi.org/10.3389/fmicb.2018.00855.
32. Sun B, Zhang M, Shen J, He Z, Fatehi P, Ni Y. Applications of cellulose-based materials in sustained drug delivery systems. Curr Med Chem. 2019;26(14):2485–2501. https://doi.org/10.2174/0929867324666170705143308.

33. Amin MK, Boateng JS. Comparison and process optimization of PLGA, chitosan and silica nanoparticles for potential oral vaccine delivery. Ther Deliv. 2019;10(8):493–514. https://doi.org/10.4155/tde-2019-0038.
34. Tiwari G, Tiwari R, Sriwastawa B, Bhati L, Pandey S, Pandey P, Bannerjee SK. Drug delivery systems: An updated review. Int J Pharm Investig. 2012;2(1):2–11. https://doi.org/10.4103/2230-973X.96920.
35. Mohammed MA, Syeda JTM, Wasan KM, Wasan EK. An overview of chitosan nanoparticles and its application in non-parenteral drug delivery. Pharmaceutics. 2017;9(4):53. https://doi.org/10.3390/pharmaceutics9040053.
36. Lee ST, Mi FL, Shen YJ, Shyu SS. Equilibrium and kinetic studies of copper(II) ion uptake by chitosan-tripolyphosphate chelating resin. Polymer. 2001;42(5):1879–1892. https://doi.org/10.1016/S0032-3861(00)00402-X.
37. Gan Q, Wang T, Cochrane C, McCarron P. Modulation of surface charge, particle size and morphological properties of chitosan-TPP nanoparticles intended for gene delivery. Colloids Surf B Biointerfaces. 2005;44(2–3):65–73. https://doi.org/10.1016/j.colsurfb.2005.06.001.
38. Tsai ML, Chen RH, Bai SW, Chen WY. The storage stability of chitosan/tripolyphosphate nanoparticles in a phosphate buffer. Carbohydr Polym. 2011;84(2):756–761. https://doi.org/10.1016/j.carbpol.2010.04.040.
39. Bayat A, Larijani B, Ahmadian S, Junginger HE, Rafiee-Tehrani M. Preparation and characterization of insulin nanoparticles using chitosan and its quaternized derivatives. Nanomedicine. 2008;4(2):115–120. https://doi.org/10.1016/j.nano.2008.01.003.
40. Vega E, Egea MA, Valls O, Espina M, García ML. Flurbiprofen loaded biodegradable nanoparticles for ophthalmic administration. J Pharm Sci. 2006;95(11):2393–2405. https://doi.org/10.1002/jps.20685.
41. Chakraborty SP, Sahu SK, Pramanik P, Roy S. In vitro antimicrobial activity of nanoconjugated vancomycin against drug-resistant Staphylococcus aureus. Int J Pharm. 2012;436(1–2):659–676. https://doi.org/10.1016/j.ijpharm.2012.07.033.
42. Arulmozhi V, Pandian K, Mirunalini S. Ellagic acid encapsulated chitosan nanoparticles for drug delivery system in human oral cancer cell line (KB). Colloids Surf B Biointerfaces. 2013;110:313–320. https://doi.org/10.1016/j.colsurfb.2013.03.039.
43. Takahashi T, Imai M, Suzuki I, Sawai J. Growth inhibitory effect on bacteria of chitosan membranes regulated by the deacetylation degree. Biochem Eng J. 2008;40(3):485–491. https://doi.org/10.1016/j.bej.2007.11.021.
44. Fathallh AA, Mahmood MA. The estimation of the viable count of *mutans streptococcus* in waterpipe smokers and cigarette smokers. J Bagh Coll Dent. 2021;33(3):23–29. https://doi.org/10.26477/jbcd.v33i3.2950.
45. Al-Bazaz FA, Radhi NJ, Abed Hubeatir K. Sensitivity of *Streptococcus mutans* to selected nanoparticles (in vitro study). J Bagh Coll Dent. 2022;34(1):20–27. https://doi.org/10.26477/jbcd.v34i1.3102.
46. Ibrahim SW, Al-Nakkash WA. Mechanical evaluation of nano hydroxyapatite, chitosan, and collagen composite coating compared with nano hydroxyapatite coating on commercially pure titanium dental implant. J Bagh Coll Dent. 2017;29(2):42–48. https://doi.org/10.12816/0038748.
47. AI-Mizraqchi AS. Effect of mouth rinse of chlorhexidine on the occurrence of the cariogenic microorganisms. IHJPAS. 2017;21(4):31–34. https://jih.uobaghdad.edu.iq/index.php/j/article/view/1426.

48. Abdul Sattar BA, Hassan A, Hassan A. In vitro antimicrobial activity of Thymus vulgaris, Origanum vulgare and Rosmarinus officinalis against dental caries pathogens. IHJPAS. 2017;25(2):1–8. https://jih.uobaghdad.edu.iq/index.php/j/article/view/610.